Effects on Buildings of Surface Curvature Caused by Underground Coal Mining

Haifeng Hu*, Xugang Lian & Shengyun Chen

College of Mining Engineering, Taiyuan University of Technology,
Taiyuan, Shanxi 030024, China
*E-mail: tyhhf65@163.com

Abstract. Ground curvature caused by underground mining is one of the most obvious deformation quantities in buildings. To study the influence of surface curvature on buildings and predict the movement and deformation of buildings caused by ground curvature, a prediction model of the influence function on mining subsidence was used to establish the relationship between surface curvature and wall deformation. The prediction model of wall deformation was then established and the surface curvature was obtained from mining subsidence prediction software. Five prediction lines were set up in the wall from bottom to top and the predicted deformation of each line was used to calculate the crack positions in the wall. Thus, the crack prediction model was obtained. The model was verified by a case study from a coalmine in Shanxi, China. The results show that when the ground curvature is positive, the crack in the wall is shaped like a "V"; when the ground curvature is negative, the crack is shaped like a "∧". The conclusion provides the basis for a damage evaluation method for buildings in coalmine areas.

Keywords: *assessment of risk of building damages; influence function; mining subsidence; surface curvature; underground coal mining.*

1 Introduction

Underground coal mining causes movement and deformation of strata and the ground. Buildings located in affected areas could be damaged by such phenomena. After underground coal is extracted, goaf is formed, the overlying strata moves to the goaf, the movement transfers to ground, and a surface subsidence basin is formed. Different locations of the subsidence basin exert varying degrees of damage to buildings or structures. For example, ground locations near the boundaries of the goaf experience maximum damage, whereas locations above the center of the goaf experience minimum damage. The causes of such phenomena are the different magnitudes of ground deformation at various positions of the subsidence basin. In mining subsidence engineering, the main indexes of deformation include subsidence, tilt, curvature, horizontal displacement and horizontal strain. The former three are vertical and the latter two are horizontal. Among these indexes of deformation, buildings on

Received May 2nd, 2016, Revised June 6th, 2016, Accepted for publication June 22nd, 2016.
 ISSN: 2337-5779, DOI: 10.5614/j.eng.technol.sci.2016.48.3.2

the ground are highly sensitive to ground curvature. At different locations of the subsidence basin, both the signs and the magnitude of ground curvature have corresponding spatial distribution characteristics. Therefore, the co-relationship between ground curvature and building deformation should be investigated.

2 State of the Art

Numerous studies have been conducted on the relationship between building deformation and subgrade deformation induced by underground coal mining and some scholars have partially studied this topic by employing field data analysis and theoretical modeling. Helmut Kratsch analyzed the effect of ground deformation on structures, including the types of stress on structures, the stress–strain behavior of soils, the earth pressure on a foundation sidewall, the friction forces acting on the structure, the changes in base pressure resulting from ground curvature [1]. Zhang Junying studied subgrade reaction under the condition of fully mechanized caving coal mining. The variations in subgrade reaction under such a condition can be divided into three stages: static stage before mining, steeply changing during mining, and slowly changing during post-mining [2].

In China, stress data of house subgrade have been obtained via observations in the Fengfeng coal area in Hebei province, the Xuzhou coal area in Jiangsu province, and the Yangquan coal area in Shanxi province. However, the mathematical relation between subgrade stress and ground deformation is yet to be established. On the basis of the analysis of the deformation data of buildings and the ground, the pressing region and pressure-release region of the house affected by mining subsidence have been proposed. According to Winkler's assumption, the empirical expression of subgrade reaction distribution was derived. This expression is affected by ground positive and negative curvature; the position of maximum subgrade reaction was indicated [3]. Tan Zhixiang and Deng Kazhong used field data to establish the formulas between building deformation and ground deformation; the formulas between cracks in buildings and ground curvature and horizontal strain have been proposed as well [4]. Ren Gang established a surface strain model based on the generalized influence function method, and the functional relationship between the surface displacement and the surface stress was obtained [5].

The result of underground displacement may cause ground movement, which in turn can be detrimental to masonry buildings, especially in hard coal regions. Thorough familiarity with general and regional characteristics of an affected area can assist reduction of the effects. The study from reference [6] identified the effects of mining subsidence on masonry buildings in the mining area of Kozlu, Zonguldak, Turkey and illustrated them with select images of damaged

masonry buildings. A framework was proposed for applying the classification and regression tree theory (CART) to assess the concrete building damage caused by surface deformation. The research introduced CART to determine the risk of building damage, with the emphasis on the grade of building damage. Given that the presented method is based on observations of damage from the previous subsidence, the method can be applied to any local conditions in which the previous subsidence is known [7]. Malinowska employed a fuzzy inference method coupled with GIS to enable the integration of diverse factors that affect risk such as surface deformations and resistance of building objects, with consideration of data uncertainty and subjectivity of evaluation of experts that make the assessment. The advantages of fuzzification were presented in the example of building data subjected to the impact of mining in a Polish mining area [8]. Zdeněk Kaláb and Markéta Lednická proposed a methodology that is part of an expert evaluation and is based on a compilation of four significant effects: local subsurface geology, groundwater table, surface deformation caused by mining and landslides. Different values of specified significances were assigned to all four selected effects. The class of foundation conditions was selected based on the summary of values of specified significances for a given point. This value describes how the selected parameters influence the vibration effect on the surface and the resistance of buildings to this seismic loading [9].

Huabin Chai studied the deformation and stability of building foundations in mining subsidence areas. A probability integral method was used to establish the further deformation formulas for building foundations in mining subsidence areas. Monitoring data from ground observation stations were applied to invert the further deformation-predicting parameters and the surface's further deformations of each coal goaf. The whole surface's further deformations were calculated by utilizing a superposition method. Additional foundation deformations, geological structures and so on were comprehensively considered [10]. Jianbing Yu analyzed the main components of proposed buildings via the finite element software ANSYS. The internal force of the main components changes the first floor under surface deformation less than without surfaced formation. The result revealed that under large surface deformation, the internal force in the beam and the column considerably changed. The beam force increased significantly by more than 100% and the column force increased significantly by more than 500%. The greatest impact of residual deformation was on the underground floor and the first floor, and then on the second and third layers. This study could provide a certain design reference for using the subsidence area of Shanxi [11]. Marian Marschalko, Işık Yilmaz and Karel Kubečka proposed a map of a possible area use for planned built-up area purposes in areas affected by underground mining-related subsidence. The outcome were three area categories in which mining subsidence affects surface

development, namely: low influence on the planned development, economically acceptable influence on the planned development, and extreme influence with prohibited development [12].

Andrzej Kowalski and Eligiusz Jędrzejec studied two deformation indicators, namely, inclination and curvature. They found that separate deformation indicators could damage the hazard assessment of building objects if their standard variation of fluctuation is well determined. Consequently, the confidence intervals of fluctuation for all separate deformation indicators can be determined. Even in a case in which the predicted separate curvatures have low values, their values can be significantly higher when their natural dispersion is considered [13]. Haifeng Hu and Xugang Lian studied a prediction model of ground damage degree under two special geological conditions: (1) thick unconsolidated soil layer and thin bedrock; (2) thin soil layer and thick bedrock. The rules for ground movement and deformation for different soil layer to bedrock ratios were obtained. Based on these rules, a prediction model of the modified parameter was proposed; this model is suitable for different values of unconsolidated soil layer thickness. The prediction results were verified with the use of two sets of typical field data [14-15].

Many studies have been conducted on the relations between surface deformation and wall deformation, some of which focused on field data, while others focused on theoretical analysis. These works have attained many notable achievements. However, limited research is available on prediction models of wall deformation caused by ground deformation. Although statistics and mechanics methods have been utilized, studies on this issue remain insufficient; that is, they cannot directly transfer the ground movement to internal walls or any parts of the buildings. Thus, this paper focuses on prediction models for the deformation and cracking of walls; the proposed models cannot only transfer the ground curvature to the wall deformation but also transform the cracks in the wall.

The remainder of this paper is organized as follows. The methodologies, including deformation prediction and crack prediction with regards to walls, are described in Section 3. The results are analyzed and discussed in Section 4. The drawn conclusions are summarized in Section 5.

3 Methodology

3.1 Prediction Model of Wall Deformation

3.1.1 Prediction Principle

The goaf formed by underground coal mining can cause ground subsidence, which in turn can cause the deformation of building foundations and even the destruction of buildings. To study the relationship between the deformation degrees of the ground and the level of damage to buildings, scholars have established the following empirical Eq. (1) [16]:

$$W_{\text{building}} = A \cdot W_{\text{ground}} - B \tag{1}$$

where:
$W_{building}$ – subsidence of building in mm
W_{ground} – subsidence of ground in mm
A – stiffness coefficient of building
B – constant of geological environment.

Eq. (1) is easy to use and calculate, but it cannot accurately reflect the effect of ground deformation on buildings; it is achieved by a similar material simulation experiment.

However, curvature, tilt and horizontal strain are the most sensitive factors in buildings. It is insufficient to calculate deformation or cracks in buildings based on ground subsidence. Thus, a new prediction model of wall deformation based on ground curvature was established.

The principle map of the prediction model is shown in Figure 1. The figure reveals that the condition of the ground positive curvature is a convex surface, which can cause changes in the contact surface between the foundation and the building. The middle of the foundation plays a supporting role, while both ends are hanging. For negative curvature, which is a concave surface, both ends play a supporting role, while the middle part is hanging.

The hypotheses for the prediction model are:

1. The wall's material, which is isotropic, nonlinear elastic, is a homogeneous medium; the deformation of the wall is in continuity.
2. The change of the surface curvature is equivalent to a supposed goaf induced by foundation non-uniform settlement.

A prediction model for mining subsidence based on the influence function is shown in Figure 2. The goaf is composed of several extracted elements and if the extracted thickness is standard unit "1", the subsidence $W_u(x)$ for x in horizontal coordinates of the surface point is induced by mining range s from 0 to +∞, which is the condition of semi-infinite extraction.

If the horizontal coordinate of the mining element is s and the horizontal coordinate of an arbitrary A is x, then the subsidence formula of semi-infinite extracting one standard unit of coal thickness can be expressed with Eq. (2):

$$W_u(x) = \int_0^{\infty} W_e(x-s)\,ds = \int_0^{\infty} \frac{1}{r} e^{-\pi \frac{(x-s)^2}{r}}\,ds \tag{2}$$

where:
$W_u(x)$ – subsidence undiced by semi-infinite extraction of one standard unit of coal thickness
$W_e(x-s)$ – subsidence of arbitrary point A(x) induced by element s
r – main influence radius.

Under the condition of element extraction, the movement and deformation of rocks are small, and continuous distribution occurs; the volume of the rock does not change. Through derivation, the horizontal movement $U_u(x)$ of an arbitrary point A induced by semi-infinite extracting of one unit coal thickness can be obtained as shown in Eq. (3):

$$U_u(x) = be^{-\pi \frac{x^2}{r}} \tag{3}$$

where:
b – horizontal movement coefficient.

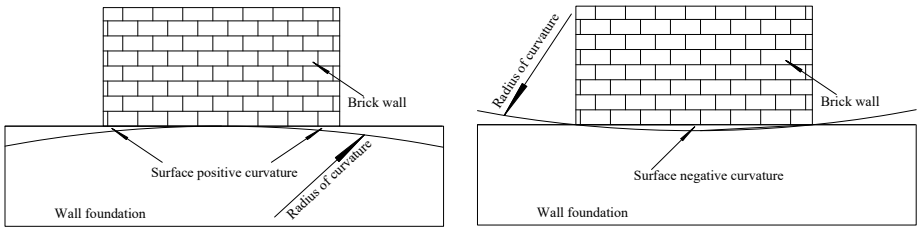

Figure 1 A perpend wall affected by ground curvature.

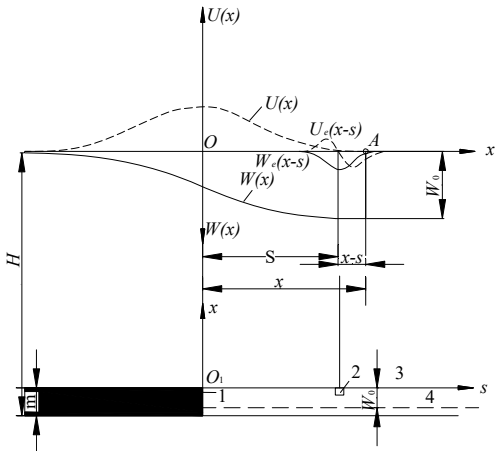

1 – coal rib; 2 – mining element; 3 – original position of the roof
4 – position of the roof after extraction; W_0 – subsidence of the roof

Figure 2 Ground subsidence and horizontal movement by semi-infinite extraction.

If the extraction thickness is *m*, not standard unit "1", the maximum subsidence of the coal seam should be $mq\cos\alpha$, which is affected by the overlying strata's broken caving and the inclined angle of the coal seam. Under this condition Eq. (4) gives

$$W(x) = W_0 \cdot \int_0^{\infty} \frac{1}{r} e^{-\pi \frac{(x-s)^2}{r}} ds \tag{4}$$

where:
$W(x)$ – subsidence of arbitrary point A induced by semi-infinite extracting coal thickness *m*
$W_0 = mq\cos\alpha$
q – subsidence coefficient
α – inclined angle of coal seam.

The horizontal movement $U(x)$ of arbitrary point A induced by semi-infinite extracting of coal thickness *m* can be obtained as shown in Eq. (5).

$$U(x) = bW_0 e^{-\pi \frac{x^2}{r}} \tag{5}$$

where the meanings of the variables are the same as above.

3.1.2 Coordinate Systems of the Prediction Model

1. *Positive curvature of the ground*

The coordinate system of the prediction model under the condition of a positive curvature can be established as shown in Figure 3. For the subsidence and horizontal displacement coordinate system, the upper-left corner of the wall is the original point *o*, and the *X*-axis is along the top line of the wall toward the right corner. The vertical axis for *W* (*x*) is pointed downward and the vertical axis for horizontal movement *U* (*x*) is pointed upward.

For the goaf coordinate system, the bottom-left corner of the wall is the original point *o1* and the horizontal axis *s* along the bottom line of the wall toward the right, and the vertical axis is pointed upward. In Figure 3, the scales of *x*, *s*, and the *Z*-axis are the same and the axes for *W* (*x*) and *U* (*x*) are magnified. The positive curvature makes the ground a convex sphere; the radius of the sphere is the reciprocal of the curvature deformation (See Eq. (6)).

$$R = \frac{1}{k(x)} \tag{6}$$

where:
$k(x)$ – curvature in the middle of foundation
R – radius of the sphere.

In Figure 3, the surface positive curvature forms two separate goafs under the wall, i.e. shapes *abc* and *cde*, which can be used as integral areas for the prediction model.

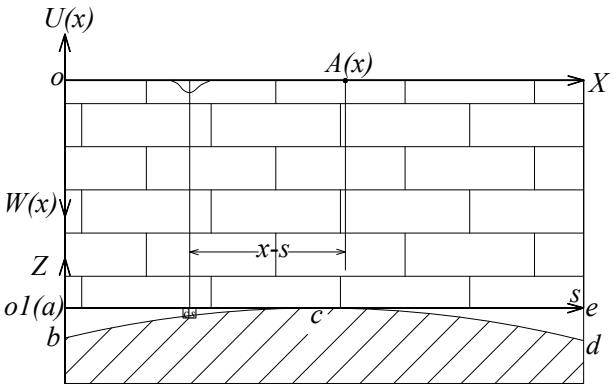

Figure 3 "Goaf" formed by ground positive curvature.

2. *Negative curvature of the ground*

The two coordinate systems under the condition of negative curvature, i.e. the subsidence and horizontal movement system and the goaf system, are similar to those under the condition of positive curvature. The difference is that under the condition of positive curvature, two separate goafs are formed. However, for the condition of negative curvature in Figure 4, one goaf under the wall was formed and the integral area is shape *abc*. The negative curvature makes the ground form a concave sphere. The relation between the radius of the sphere and the negative curvature conforms to Eq. (6) as well.

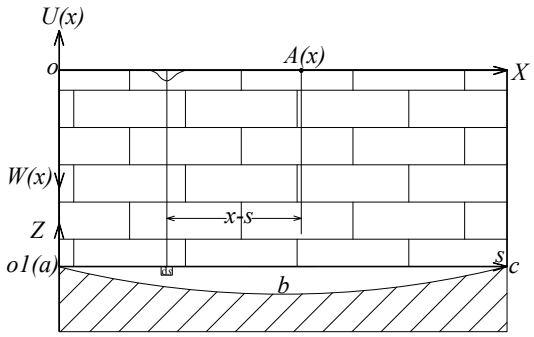

Figure 4 "Goaf" formed by ground negative curvature.

3.1.3 Calculation Formulations

1. *Positive curvature*

As shown in Figure 5, under the condition of ground positive curvature, the whole integral region shapes *abc* and *cde* are divided into horizontal layers of number *N*. Here, *m* is the vertical distance of *ab* or *ed*, the height for each layer is *m*/*N*, so the vertical distance from *c* to layer *i* is $\frac{m}{N}\cdot i$, and the chord length in layer *i* is given by Eq. (7):

$$d_i = 2\sqrt{\frac{m}{N}\cdot i\cdot(2R-\frac{m}{N}\cdot i)} \tag{7}$$

Subsidence $W_i(x)$ and horizontal movement $U_i(x)$ at x of the horizontal axis induced by layer *i* in Eqs. (8) and (9) can be calculated as follow:

$$W_i(x) = W_0^i\cdot\left\{\begin{matrix} W_u(x)-W_u(x-l+d_i/2) \\ +W_u(x-l-d_i/2)-W_u(x-L)\end{matrix}\right\} \tag{8}$$

$$U_i(x) = W_0^i \cdot \left\{ \begin{matrix} U_u(x) - U_u(x - l + d_i/2) \\ +U_u(x - l - d_i/2) - U_u(x - L) \end{matrix} \right\} \tag{9}$$

where:

$W_0^i = \frac{m}{N} \cdot q$ is the maximum subsidence of layer *i*

$l = L/2$ is the half-length of the wall

d_i and the other variables are the same as above

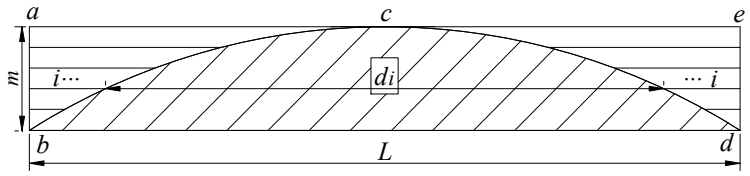

Figure 5 Dividing the integral area for positive curvature.

In the integral region, subsidence W(*x*) and horizontal movement *U*(*x*) of the point *x* along the horizontal axis of the wall are calculated by the integral superposition principle (see Eqs. (10) and (11)), and the calculation formula for positive curvature is:

$$W(x) = \sum_{i=1}^{N} W_i(x) \tag{10}$$

$$U(x) = \sum_{i=1}^{N} U_i(x) \tag{11}$$

2. *Negative curvature*

As shown in Figure 6, under the condition of ground negative curvature, the completely integral region *abc* is divided into N layers. With the use of the same algorithm, the chord length in layer *i* can be obtained as

$$d_i = 2\sqrt{m(1 - \frac{i}{N})(2R - m + \frac{m}{N} \cdot i)} \tag{12}$$

Subsidence $W_i(x)$ and horizontal movement $U_i(x)$ at *x* of the horizontal axis induced by layer *i* are as shown in Eqs. (13) and (14).

$$W_i(x) = W_0^i \cdot \left\{ W_u(x - l + d_i/2) - W_u(x - l - d_i/2) \right\} \tag{13}$$

$$U_i(x) = W_0^i \cdot \left\{ U_u(x - l + d_i/2) - U_u(x - l - d_i/2) \right\} \tag{14}$$

where d_i is calculated by Eq. (12), and the other variables are the same as above.

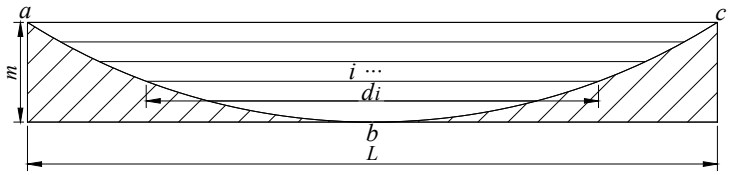

Figure 6 Dividing the integral area for negative curvature.

Thus, under the condition of ground negative curvature and by using the integral superposition principle, subsidence $W(x)$ and horizontal movement $U(x)$ of point x along the horizontal axis of the wall are calculated via Eqs. (10) and (11).

3.1.4 Program Developed

The C# language was used to realize the automatic calculation of the deformation of the perpend wall. The detailed processes are as follow:

1. The positive or negative curvature is obtained by a software application for mining subsidence prediction [17].
2. The prediction parameters and the size of the perpend wall need to be inputted. The interface is shown in Figure 7.

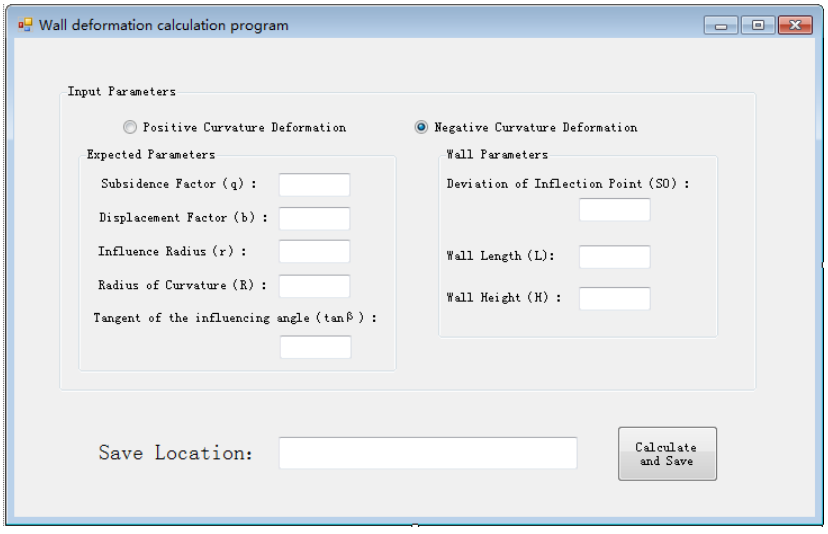

Figure 7 Program interface.

3.2 Crack Prediction Model

When the wall is subjected to a tensile deformation that is larger than the critical value, a crack will form in the wall. In the model, the deformation value of the wall mainly includes the horizontal movement and the subsidence. The direction of subsidence is vertical to down, so the occurrence of cracks is mainly due to horizontal movement. The critical value for wall cracking is calculated based on horizontal movement, as shown in Figure 8.

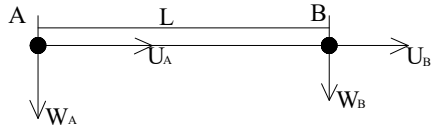

Figure 8 Mechanism analysis of wall cracking.

Assuming that line AB is along the wall, the length of AB is L before being affected by deformation. After being affected, the subsidence of point A is W_A, the horizontal movement of point A is U_A, the subsidence of point B is W_B and the horizontal movement of point B is U_B. The movement vector of point A along the horizontal direction is

$$\mathrm{R}_A = U_A \tag{15}$$

The movement vector of point B along the horizontal direction is

$$\mathrm{R}_B = U_B \tag{16}$$

The deformation of AB in the length direction according to Eqs. (15) and (16) is given by Eq. (17).

$$\Delta L = \mathrm{R}_B - \mathrm{R}_A \tag{17}$$

Then, the strain of AB is given by Eq. (18).

$$\varepsilon_L = \frac{\Delta L}{L} = \frac{\mathrm{R}_B - \mathrm{R}_A}{L} = \frac{U_B - U_A}{L} \tag{18}$$

If ε_L is larger than a critical value, then a crack will be formed. The critical value can be obtained by Eq. (19).

$$\varepsilon_0 = 2 \cdot \left(1 - \mu^2\right) \cdot \mathrm{C} \cdot \tan\left(45° + 0.5 \cdot \varphi\right) / \mathrm{E} \tag{19}$$

where μ is Poisson's ratio, C is the cohesion, φ is the internal friction angle, and E is the elastic modulus.

When calculating the critical deformation of the wall, $\mu = 0.3, \mathrm{C} = 8 \times 10^7\ \mathrm{N/m^2}$, $\varphi = 30°, \mathrm{E} = 3 \times 10^{10}\ \mathrm{N/m^2}$ are taken into Eq. (19), and the critical value ε_0 = 6mm/m can be determined.

The crack width of line AB is calculated by

$$\Delta D = \varepsilon_L - \varepsilon_0 \tag{20}$$

Eq. (20) is the prediction model of wall cracking, where ΔD is the crack width within a length of 1 m. When $\Delta L < 0$, the deformation of the wall is in compression and a crack will not be formed.

The criterion for the possibility and size of the crack is set by Eq. (18). When the horizontal strain of AB is negative, then AB is in compression and a crack will not be formed. However, when the horizontal strain of AB is positive and larger than the critical value, a crack will be formed.

Four observation lines are set up on the wall to study the deformation of the wall under the conditions of surface curvature. The heights of the observation lines from the ground are 5, 10, 15, and 20 m. The horizontal strain of each line is calculated. The crack positions in the wall are analyzed.

4 Result Analysis and Discussion

4.1 Prediction Model of Wall Deformation

The relationship between surface curvature and damage levels of buildings in China is shown in Table 1. The ground curvature radius of 5000 m corresponds to damage level A, radius 2500 m corresponds to damage level B, radius 1600 m corresponds to damage level C, and radius 1250 m corresponds to damage level D. Based on a wall in a brick-concrete structure, the prediction parameters can be selected as: coefficient of subsidence $q = 0.5$, length of building $L = 50$ m, height of building $H = 20$ m, and main influence radius $r = 10$ m.

Under the condition of ground positive curvature, Tabel 1 and Section 3.1.2 are referenced, so the maximum mining height of damage level A corresponds to 0.245 m, level B to 0.49 m, level C to 0.77 m, level D to 0.98 m. Under the condition of ground negative curvature, the maximum mining height for damage level A is 0.125 m, for level B it is 0.25 m, for level C it is 0.39 m, for level D it is 0.50 m.

Table 1 Damage levels of brick masonry buildings.

Damage levels	Deformation of ground			Damage Classification	Solving Methods
	Horizontal strain	Curvature	Tilt		
A	≤ 2.0	≤ 0.2	≤ 3.0	Almost imperceptible Slight	No repair Simple repair
B	≤ 4.0	≤ 0.4	≤ 6.0	Minor	Minor repair
C	≤ 6.0	≤ 0.6	≤ 10.0	Moderate	Moderate repair
D	> 6.0	> 0.6	> 10.0	Serious Profoundly serious	Heavy repair Rebuild

4.1.1 Ground Positive Curvature

When the ground deformation has a positive curvature, the deformation results of a perpend wall are as shown in Figure 9.

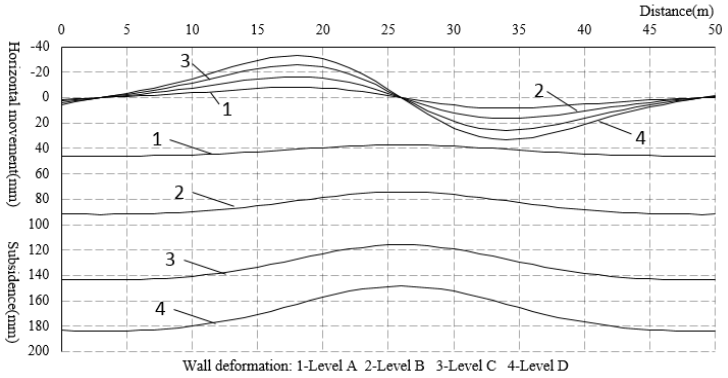

Figure 9 Deformation results of wall in ground positive curvature.

Based on the calculation results and curves, the deformation of the wall is symmetrical and some conclusions can be obtained:

1. The middle part of the foundation of the wall plays a supporting role and reduces subsidence. At this point, the horizontal displacement is zero, the interaction force between the foundation and the subgrade is large, and a stress concentration area is formed.
2. At the ends of the wall, the subsidence values reach the maximum and they are located above the goaf.
3. On both sides of the wall, the pressure is reduced and corresponds to the tensile deformation.
4. The deformation of the wall is proportional to the ground curvature.

4.1.2 Ground Negative Curvature

Figure 10 shows the deformation results of a perpend wall when the ground curvature is negative. The deformation features of the wall caused by ground negative curvature are as follows.

1. The supporting points of the foundation are located at the ends of the wall and the stress is concentrated in these two areas as well. The middle area of the wall is in the condition of stress unloading, thereby causing the middle of the wall to subside.
2. The top horizontal line of the wall is in compression and cracks are difficult to form in this part.
3. At the same magnitude of ground curvature and a degree of deformation occurring in the wall, a positive curvature is much larger than a negative curvature. The reason is that the compressive capacity of a brick-masonry structure is much greater than the tensile strength.

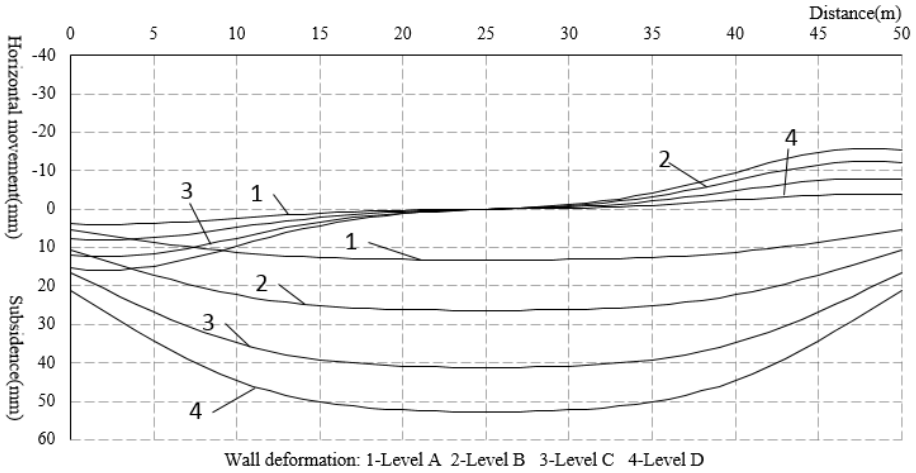

Figure 10 Deformation results of wall in ground negative curvature.

4.2 Discussion of Crack Prediction Results

4.2.1 Ground Positive Curvature

The curves of horizontal strain for the top line of the wall are shown in Figure 11. The curves of the horizontal strain of the four observation lines set up as described above are shown in Figure 12 under a ground curvature of 0.4 mm/m.

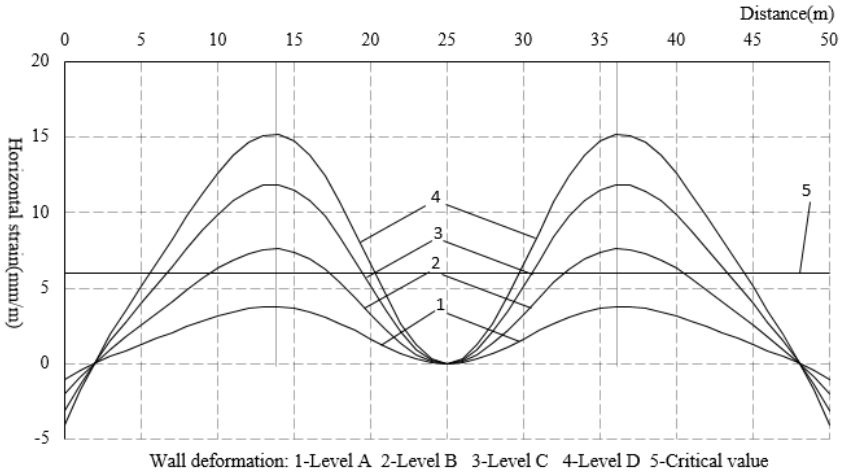

Figure 11 Horizontal strain for the top line of the wall (positive curvature).

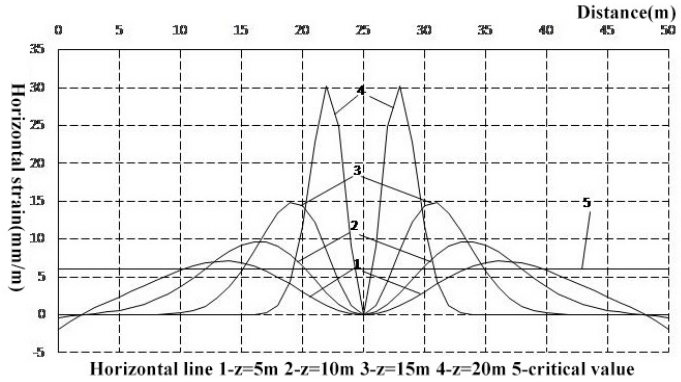

Figure 12 Horizontal strain for four observation lines on the wall (positive curvature).

Based on Figures 11 and 12, certain conclusions can be obtained:

1. When the wall is under the condition of ground positive curvature, the horizontal strain is positive; this result indicates that the wall is stretched and reaches up to the maximum points at the ends of wall. The ground curvature is proportional to the horizontal strain and the tensile strength.
2. When the wall is subjected to level A damage, the maximum crack width is 1-2 mm, which is calculated by Eq. (20). When the wall suffers level B damage, the maximum crack width is 9-10 mm. The crack width for level C damage is 18-20 mm, and the crack width of level D damage is more than

20 mm. Damage level A – curvature value 0.2 mm/m^2 – radius of curvature 5000 m – mining height 0.125m; damage level B – curvature value 0.4 mm/m^2 – radius of curvature 2500 m – mining height 0.25 m; damage level C – curvature value 0.6 mm/m^2 – radius of curvature 1600 m – mining height 0.39 m; damage level D – curvature value 0.8 mm/m^2 – radius of curvature 1250 m – mining height 0.50 m.

3. Based on Figure 12, the closer to the ground the observation line is, the greater the deformation value, viz. the bottom deformation of the wall is larger than the upper. The crack locations for each observation line are apparent in the wall; the crack regions are shown in Figure 13. Considering the effect of contact surface between the wall and the foundation, the angle between the crack and the horizontal line is 59°; the overall shape is that of a "V".

The horizontal strains of four horizontal lines z = 5 m, z = 10 m, z = 15 m and z = 20 m were calculated by Eq. (18) and are shown in Figure 12. When the value of horizontal strain exceeds critical value 6 mm/m, a crack in the wall will be formed. Crack boundary points between horizontal lines are connected by straight lines and the crack area will be formed as shown in Figure 13. The acute angle between the boundary line of the crack area and the horizontal line is 59°. Under the condition of negative curvature, the acute angle of 53° in Figure 16 can be determined by the above method.

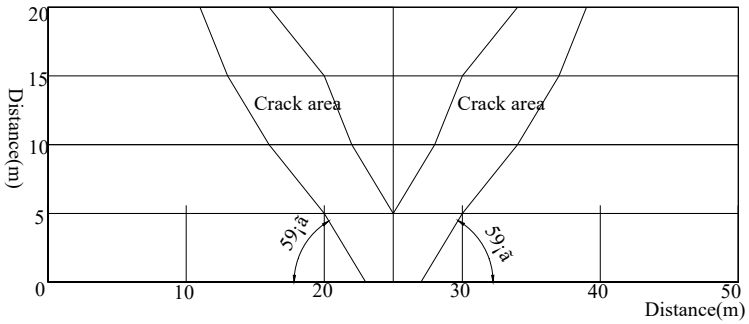

Figure 13 Cracks in the wall (positive curvature).

4.2.2 Negative Curvature of Ground

The curves of horizontal strain for the top line of the wall are shown in Figure 14. The curves of the horizontal strain of the four observation lines set up on the wall are shown in Figure 15 under a ground curvature of -0.4 mm/m. Based on Figure 15, (1) when the wall is under the condition of ground negative curvature, the horizontal strain is negative, which indicates that the deformation

of the wall is in compression; (2) the curvature of the surface is proportional to the horizontal compression of the wall; and (3) considering the effect of contact surface between wall and ground, the crack appears in a "∧" shape as shown in Figure 16, and the angle with the horizontal line is approximately 53°.

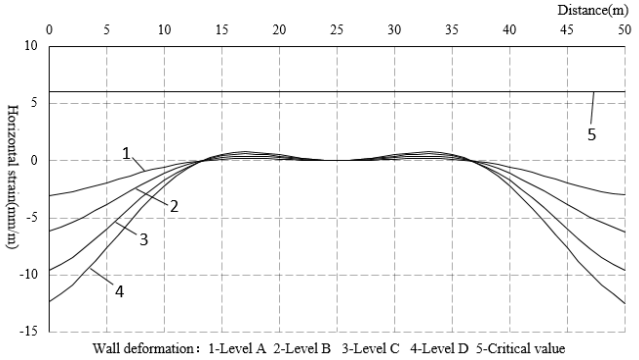

Figure 14 Horizontal strain for the top line of the wall (negative curvature).

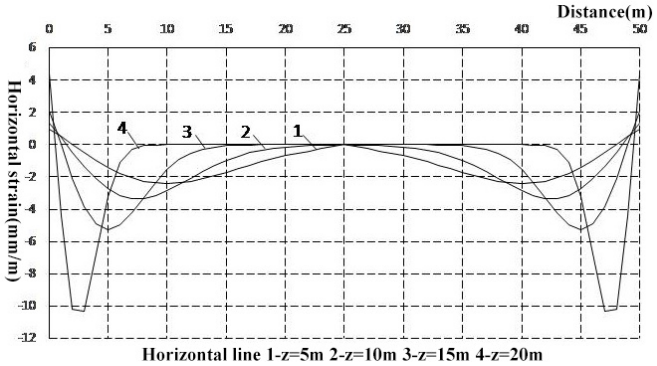

Figure 15 Horizontal strain for four observation lines on the wall (negative curvature).

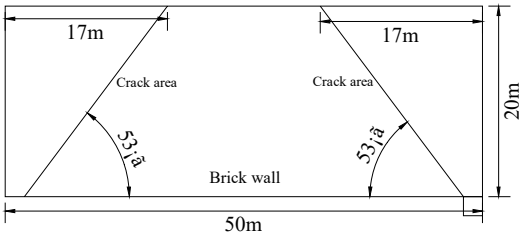

Figure 16 Cracks in the wall (negative curvature).

4.3 Case Study

In May 2014, a house damaged by underground coal mining, located in southern Shanxi, China, was investigated. This house is shown in Figure 17; the house was relocated in 2013. The location, the cracks and the size of the wall have been recorded. Figure 18 shows the corresponding map of the ground and the underground mining plane.

The extraction year of the panel was 2013, the length of the coal panel was 574 m, the inclined length was 128 m, the mining depth was 160 m, the thickness of the coal seam was 1.8 m, the coal seam was approximately horizontal, the overlying strata thickness was roughly 150 m and the loess thickness was 10-60 m. The village was located above the north edge of the extracted area. The entire village suffered from tensile strain and the ground curvature in this village was positive.

Figure 17 Case study of wall cracks.

The following data were obtained from the field measurements: the wall was located at the outer edge of the goaf, the height of the wall was 2 m, the length was 5 m, the crack width was 50 mm and connected bottom-up, and the shape of the crack was a "V". The angle of the crack with the horizontal plane was 62°. Table 1 shows that the degree of damage to this house was level D. Furthermore, subsidence prediction software was applied to calculate the curvature of this house. The predicted curvature was 0.8×10^{-3}/m, so the wall could be classified as having level D damage, thereby corroborating the field investigation. Under the special condition of Figure 18, the predicted crack width based on this study was from 42-46 mm, which is close to the field value of 50 mm.

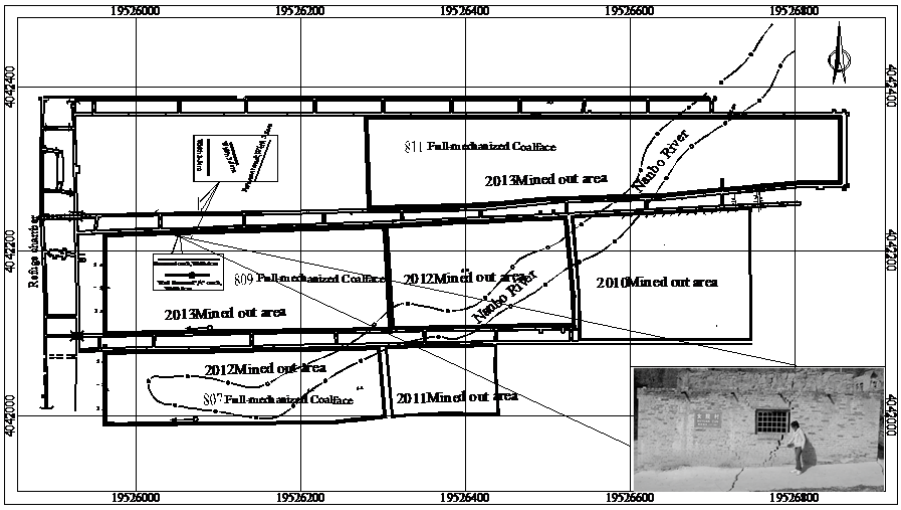

Figure 18 Corresponding map of the ground and underground of mining.

5 Conclusions

To study the effect of ground curvature caused by underground coal mining on buildings, the influence function method for mining subsidence prediction was used for wall movement prediction and a crack calculation method was proposed. Based on this research, the following conclusions can be drawn:

1. Based on the influence function method, the deformation prediction model of the curvature of the perpend wall was established and C# was used for implementation. The prediction formula for single-side wall damage was determined.
2. When the ground curvature is positive, the maximum width of the cracks at damage level B is 9-10 mm; the maximum width of the cracks at damage level C is 18-20 mm; the maximum width of the crack of damage level D is more than 20 mm. The shape of the crack appears as a "V" and the angle with the horizontal line is 61-66°. When the ground curvature is negative, the shape of the crack is a "∧" and the angle with the horizontal line is roughly 53°.

The results of this study are limited to perpend walls. In reality, a house is built with several types of walls and other structures. Thus, future studies should focus on predicting the influence of ground deformation on combined walls or structures.

Acknowledgments

Many thanks to language editor Sybrand Zijlstra, who gave a great deal of help in correcting the grammar in this paper. This study was supported by the National Natural Science Foundation of China (51574132 and 51504159) and the Natural Science Foundation of Shanxi Province, China (2014011001-3).

References

[1] Kratzsch, H., *Mining Subsidence Engineering*, New York: Berlin Heidelberg, pp. 335-362, 1983.

[2] Zhang, J.Y., *The Variation of Ground Reaction Force under the Condition of Fully Mechanized Caving Mining*, Coal Science and Technology, **36**(2), pp.23-25, 2002.

[3] Deng K.Z., Tan, Z.X., Guo, W.B. & Zhang, H.Z., *The Law of the Distribution of the Foundation of the Buildings in the Mining Area*, Journal of China University of Mining and Technology, **43**(2), pp. 95-99, 2004

[4] Tan, Z.X. & Deng, K.Z., *Research Progress of Coal Mining under Buildings*, Journal of Liaoning Technical University, **26**(4), pp. 485-488, 2006.

[5] Ren, G., Li, J. & Buckeridge, J., *Calculation of Mining Subsidence and Ground Principal Strains Using Generalized Influence Function Method*, Mining Technology, **119**(1), pp. 34-41, 2010.

[6] Can, E., Kuşcu, Ş. & Kartal, M.E., *Effects of Mining Subsidence on Masonry Buildings in Zonguldak hard coal region in Turkey*, Environmental Earth Sciences, **66**(8), pp. 2503-2518, 2012.

[7] Malinowska, A., *Classification and Regression Tree Theory Application for Assessment of Building Damage Caused by Surface Deformation*, Natural Hazards, **73**(2), pp. 317-334, 2014.

[8] Malinowska, A., *A Fuzzy Inference-based Approach for Building Damage Risk Assessment on Mining Terrains*, Engineering Structures, **33**(1), pp. 163-170, 2011.

[9] Kaláb, Z. & Lednická M., *Foundation Conditions of Buildings in Undermined Areas: An Example of Evaluation*, Acta Geophysica, **60**(2), pp. 399-409, 2012.

[10] Chai, H.B., *Study on the Deformation and Stability of Building Foundations in Mining Subsidence Areas*, Applied Mechanics and Materials, **166-169**, pp. 1967-1970, 2012.

[11] Yu, J.B., *The Influence of Main Components of Building under Residual Deformation in Subsidence Area*, Advanced Materials Research, **919-921**, pp. 477-481, 2014.

[12] Marschalko M., Yilmaz I. and Kubečka, K., Bouchal, T., Bednárik, M., Drusa, M. & Bendová, M., *Utilization of Ground Subsidence Caused by Underground Mining to Produce a Map of Possible Land-use Areas for Urban Planning Purposes*, Arabian Journal of Geosciences, **8**(1), pp. 579-588, 2015.

[13] Kowalski, A. & Jędrzejec, E., *Influence of Subsidence Fluctuation on The Determination of Mining Area Curvatures*, Archives of Mining Sciences, **60**(2), pp. 487-505, 2015.

[14] Hu, H.F. & Lian, X.G., *Subsidence Rules of Underground Coal Mines for Different Soil Layer Thickness: Lu'an Coal Base as an Example*, International Journal of Coal Science & Technology, **2**(3), pp. 178-185, 2015.

[15] Hu, H.F., Lian, X.G. & Li, Y., *Physical Experiments on the Deformation of Strata with Different Properties Induced by Underground Mining*, Journal of Engineering Science and Technology Review, **9**(1), pp. 74-80, 2016.

[16] Tan, Z.X. & Deng, K.Z., *Simulation Study on Dynamic Deformation Law of Buildings in Mining Area*, Journal of Xi'an University of Science And Technology, **26**(3), pp. 349-352, 2006.

[17] Han, K.F., Kang, J.R., Wang, Z.S. & Wu, K., *Mountain Mining Dynamic Surface Crack Prediction Method*, Journal of Mining & Safety Engineering, **31**(6), pp. 896-900, 2014.